2015 European Control Conference (ECC)
July 15-17, 2015. Linz, Austria

Sloshing-aware attitude control of impulsively actuated spacecraft

Pantelis Sopasakis[a], Daniele Bernardini[a,c], Hans Strauch[b], Samir Bennani[d] and Alberto Bemporad[a,c]

***Abstract*— In this tutorial paper we present a novel modeling methodology to derive a nonlinear dynamical model which adequately describes the effect of fuel sloshing on the attitude dynamics of a spacecraft. We model the impulsive thrusters using mixed logic and dynamics leading to a hybrid formulation. We design a hybrid model predictive control scheme for the attitude control of a launcher during its long coasting period, aiming at minimising the actuation count of the thrusters.**

***Index Terms*— Attitude Control, Sloshing, Hybrid Model Predictive Control, Aerospace.**

I. Introduction

Upper stages of launchers sometimes have a control mode known as "long coasting phase" which can last up to five hours. The spacecraft, already in orbit with the main engine switched off, drifts with its payloads toward the point on the orbit where the separation shall take place. The stage slowly rotates around its roll axis in order to avoid heating up (*barbecue mode*). The control torques are generated by thrusters. For some types of thrusters the accepted total number of actuation is limited and the long duration of the coasting period makes this problem rather challenging.

Although the spin rate is low (1 to $5deg/sec$), the gyroscopic coupling cannot be neglected and the plant dynamics must be treated in a multiple-input/multiple-output (MIMO) fashion [1]. Sometimes the main engine will be re-ignited just prior to the payload release in order to change the orbit parameters. Therefore, considerable amount of propellant is left in the tank (up to 1 to 2 tons). Compared to the dry-mass (in the order of 4 to 6 tons) the torques generated by the propellant motion cannot be neglected (*sloshing phenomenon*).

The classical way to model the fluid motion are pendulum or spring/damper models (see *e.g.*, [2] and references therein). Such models are fairly representative if a sufficient acceleration (either from the main engine or in a gravitational field) is present. In a near zero-g environment no constant acceleration is present, which could generate the restoring force, responsible for the oscillating behavior of the fluid and the motion of the fluid is only dominated by the surface tension. Unlike these two cases the barbecue mode during the long coasting flight generates a special acceleration environment.

In the case of a cylindrical, centrally placed tank the spin rate generates, via the centrifugal force, a rotational symmetrical acceleration field. In principle, an oscillating behaviour could be expected again, however, a spinning body in free-fall condition will exhibit a motion combining the spinning around the body axis plus a slower rotation of the axis itself (nutation and precession, see [3] and Figure 1). The fluid collects as a bulge and, following the rotating acceleration vector, slowly rotates along the tank wall as it is also reported by Veldman and Vogels [4]. This motion creates large, time-varying off-diagonal elements in the inertia tensor. Computational fluid dynamics (CFD) analyses have been proposed and are best suited to model the sloshing effect, but the difficulty to perform such simulations in real time renders them unsuitable for [5]. In this paper we describe a control-oriented model in analytic form whose parameters are determined offline based on CFD computations.

A noteworthy burgeoning interest in applications of model predictive control (MPC) in aerospace and, in particular, in attitude control can be observed. The use of MPC for attitude control has been proposed by Manikonda *et al.* [6], Vieira *et al.* [7] and other authors. Hegrenæs *et al.* propose an explicit MPC control scheme for attitude control [8], [9]. Other attitude control approaches have been proposed in the literature. Simpler control solutions such as PD and LQR have also been proposed without, however, being able to take consistently into account the constraints that apply on the system [10], [11]. Nonlinear model predictive control approaches for constrained attitude control have been proposed by Kalabic *et al.* [12].

The thrusters of the spacecraft that are used to control its attitude are subject to a *minimum impulse bit*, that is, once activated they will apply a minimum torque to the spacecraft. This effect leads to a hybrid description of the dynamics of the spacecraft and, eventually, to a *hybrid MPC* problem which is formulated as a mixed-integer quadratic problem. Mixed integer programming has been used by Richards *et al.* [13] and Mellinger *et al.* [14] for offline trajectory planning. The proposed approach takes trajectory planning online and applies the control actions in a receding horizon manner.

Recent developments in optimization theory enable the design of fast embedded MPC controllers with guaranteed convergence in fixed-point arithmetic [15]. These results have made their appearance in the field of attitude control [16]. Frick *et al.* [17] proposed certain heuristics to considerably speed-up the solution of hybrid MPC optimization problems and yield near-optimal solutions. Evidently, optimization and

[a] IMT Institute for Advanced Studies Lucca, Piazza San Ponziano 6, 55100 Lucca, Italy. Emails: {pantelis.sopasakis, daniele.bernardini,alberto.bemporad}@imtlucca.it.

[b] Airbus DS, Airbus-Allee 1, 28199 Bremen, Germany. Email: hans.strauch@astrium.eads.net.

[c] ODYS Srl, via della Chiesa XXXII trav. I n. 231, 55100 Lucca, Italy.

[d] European Space Agency (ESA), Keplerlaan 1, Noordwijk, The Netherlands, Email: samir.bennani@esa.int.

In part, this work has been carried out in connection with ESA's Future Launcher Preparatory Program (FLPP) study "Upper Stage Attitude Control Design Framework" under the lead of Adriana Sirbi.

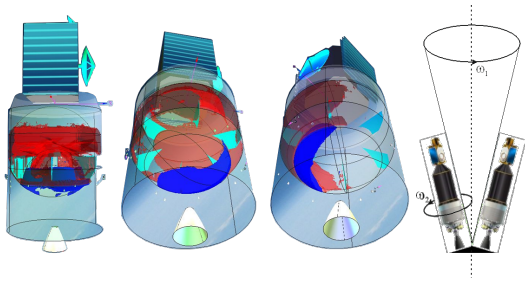

Fig. 1: CFD simulation of upper stage with two cylindrical tanks. Two types of propellant in red and blue. From left to right: (i) end of spin-up phase, started from initially flat propellant distribution, (ii) fluid is collected as a bulge, (iii) the bulge has slowly rotated with the tank, (iv) illustration of spinning and nutation; precession not shown.

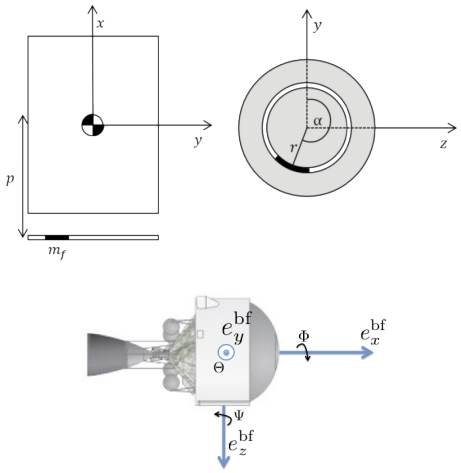

Fig. 2: (Up) Multibody model for the bulge phenomenon. The values of p and r define the circular rotation which the bulge can move (see Fig. 1) and α describe the current fluid position. (Down) Body-fixed body frame with the x-axis, defined by e_x^{bf}, aligned with the principal axis of the spacecraft.

control theory offer the tools for the use of of MPC in real aerospace applications.

In this paper we derive a state-space continuous-time model of the spacecraft attitude employing a simplified sloshing model (see Section II). The impulsive nature of the thrusters is modeled using binary variables to yield a hydrid dynamical system. In Section III, we introduce an extended Kalman filter to reconstruct the unmeasured sloshing-related states of the systems which we combine with a hybrid model predictive controller which makes use of a linearized version of the system which is updated online using estimated state information (Section IV). Finally, we provide simulation results to demonstrate the performance of the closed-loop system.

Notation. Let $\mathbb{N}$, $\mathbb{R}$, $\mathbb{R}^n$, $\mathbb{R}^{m\times n}$ be the sets of natural m-by-n matrices. Let P be a logical proposition. We denote by $[P]$ its *truth value*, *i.e.*, $[P] = 1$ if P is true and $[P] = 0$ otherwise. We use the notation $x(t)$ with $t \geq 0$ for continuous-time signals and x_k with $k \in \mathbb{N}$ for discrete-time ones. For any nonnegative integers k_1, k_2 with $k_1 \leq k_2$, the finite set $\{k_1, \dots, k_2\}$ is denoted by $\mathbb{N}_{[k_1,k_2]}$.

II. Attitude Model with Rotating Mass

In this paper we study the attitude dynamics using a body-fixed (BF) frame which is a right-handed, orthonormal reference frame fixed to the spacecraft so that the x-axis is aligned to its principal axis and the rotation about it is denoted by Φ and is called the *roll angle* [10, Sec. 1.1.2]. The rotational displacement about the y-axis defines the *pitch angle* Θ and the rotation about the z-axis is the *yaw angle* Ψ.

In this section we provide a detailed discussion on the derivation of a dynamical model that captures the upper stage attitude dynamics in light of the additional torques caused by the sloshing of fuel and the impulsive thrusters which are used to control the attitude of the spacecraft.

In the following the dynamics of motion is derived via the Lagrange formalism (see [18]). The system is modeled as a rigid body (stage plus payloads) and a ring within which a point mass m_f can rotate (see Figure 2). The parameters p, r and α are determined via CFD simulations and represent the position of the fluid within the tank for a specific spin rate.

The generalized coordinates q of the system are the angular rates $\omega = (\omega_x, \omega_y, \omega_z)$ and the propellant position α. The energy T of the system is:

$$T = \frac{1}{2}\sum_{i,j=1}^{3} J_{ij}\omega_i\omega_j + \frac{1}{2}m_f r^2\dot{\alpha}^2. \tag{1}$$

The solution of the Lagrangian equation of the system, that is $\frac{d}{dt}(\frac{\partial T}{\partial \dot{q}_i}) - \frac{\partial T}{\partial q_i} = 0$, provides the equation of motion, thus, the motion of the mass m_f is given by

$$\ddot{\alpha} = -\kappa\dot{\alpha} + \frac{\theta(\alpha,\omega)}{m_f r^2}, \tag{2}$$

where $\kappa > 0$ is a constant representing the wall friction and θ is given as

$$\begin{aligned}\theta(\alpha,\omega) = r^2(\omega_y^2 - \omega_z^2)\sin\alpha\cos\alpha + pr\omega_x\omega_y\sin\alpha \\ - pr\omega_x\omega_z\cos\alpha - r^2\omega_y\omega_z\cos(2\alpha).\end{aligned} \tag{3}$$

Equation (3) is the coupling of the main body motion onto the moving mass m_f, *i.e.*, the excitation caused by the combined motion of precession and nutation. Equation (2) is the sum of the accelerations acting on m_f and κ must be adapted such that relative motion of m_f resembles the bulge motion computed via CFD. Equation (2) can be written as

$$\dot{\alpha} = \beta, \tag{4}$$

$$\dot{\beta} = -\kappa\beta + \frac{\theta(\alpha,\omega)}{m_f r^2}. \tag{5}$$

The inertia tensor J of the upper stage is a function of the sloshing state α as $J(\alpha) = J_0 + J_{m_f}(\alpha)$, where J_0 is the inertia tensor of the spacecraft without the effect of sloshing (which is a diagonal matrix) and $J_{mf}(\alpha)$ is the

contribution of the moving mass to the overall inertia given by the symmetric matrix

$$J_{m_f}(\alpha)=m_f \begin{bmatrix} r^2 & -pr\cos\alpha & -pr\sin\alpha \\ * & p^2+r^2\sin^2\alpha & -r^2\sin\alpha\cos\alpha \\ * & * & p^2+r^2\cos^2\alpha \end{bmatrix}. \quad (6)$$

For convenience let us define

$$\Omega(\omega) = \begin{bmatrix} 0 & \omega_z & -\omega_y \\ -\omega_z & 0 & \omega_x \\ \omega_y & -\omega_x & 0 \end{bmatrix}. \quad (7)$$

The torque τ given by

$$\tau = \tau_{ext} + \Omega(\omega)\cdot l, \quad (8)$$

where $l = J\omega$ is the angular momentum and τ_{ext} is the torque applied by the thrusters. Differentiating l and by virtue of (8) and using the notation $J'(\alpha) = \mathrm{d}J/\mathrm{d}\alpha$ we have

$$\dot{l} = \dot{J}\omega + J\dot{\omega} = J'(\alpha)\dot{\alpha}\mathrm{d}t + J\dot{\omega}, \quad (9)$$

and given that $\tau = \mathrm{d}l/\mathrm{d}t$ we have that

$$\tau = J'(\alpha)\dot{\alpha}\omega + J\dot{\omega}. \quad (10)$$

The attitude dynamics, by virtue of (8) and (10), is now described by

$$\dot{\omega} = J^{-1}\Omega J\omega + J^{-1}\tau_{ext} - J^{-1}J'(\alpha)\beta\omega. \quad (11)$$

The right-hand side of (11) is a complex function of ω mainly because of the involvement of the inverse J^{-1}; its derivation in explicit form was carried out using the Symbolic Toolbox of MATLAB. The pitch and yaw errors, denoted by $\epsilon_y(t)$ and $\epsilon_z(t)$ respectively, follow the dynamics:

$$\dot{\epsilon}_y(t) = \omega_y(t) + \epsilon_z(t)\omega_x(t), \quad (12a)$$
$$\dot{\epsilon}_z(t) = \omega_z(t) - \epsilon_y(t)\omega_x(t). \quad (12b)$$

The attitude dynamics is described by the state vector $z(t) = (\epsilon_y, \epsilon_z, \omega_x, \omega_y, \omega_z, \alpha, \beta)'$ with input $u(t) = (\tau_{ext,x}, \tau_{ext,y}, \tau_{ext,z})'$. The overall dynamics given in equations (4), (11) and (12) can then be written concisely in the form

$$\dot{z}(t) = F(z(t), u(t)), \quad (13a)$$
$$y(t) = Cz(t), \quad (13b)$$

where in particular $F : \mathbb{R}^7 \times \mathbb{R}^3 \to \mathbb{R}^7$ has the input-affine form $F(z,u) = f(z) + g(z)u$ and $C \in \mathbb{R}^{5\times 7}$ is the matrix $C = [\, I_5 \; 0\,]$, *i.e.*, the sloshing states α and β cannot be measured directly in real time.

The above system is discretized with sampling period $h > 0$ to give:

$$z_{k+1} = z_k + hF(z_k, u_k), \quad (14a)$$
$$y_k = Cz_k, \quad (14b)$$

which will be used as the nominal plant model in the formulation of the state estimation and model predictive control problems in what follows. For convenience we define $f_h(z,u) = z + hF(z,u)$.

III. State Estimation & Online Linearization

We employ an extended Kalman filter (EKF) to estimate the state of the discrete-time system (14). The extended Kalman filter is the nonlinear version of the Kalman filter which makes use of the nominal nonlinear system dynamics to predict the evolution of the state while it uses updated local linearizations of the nonlinear system at the current estimated state to estimate the covariance of the state vector [19]. Here, the state estimates $\hat{z}_k$ are updated according to the nonlinear equation

$$\hat{z}_{k+1} = (I - K_k C f_h(\hat{z}_k, u_k)) + K_k y_k, \quad (15)$$

where $K_k \in \mathbb{R}^{7\times 7}$ is determined by $K_k{=}G_kC'(CG_kC' + R)^{-1}$ with $P_{k+1}{=}(I - K_kC)P_k$, and

$$F_k = \left.\frac{\partial f_h}{\partial z}\right|_{(\hat{z}_k, u_k)} \text{ and } G_k = F_kP_kF_k' + Q. \quad (16)$$

The matrix Q in the above equations is the covariance matrix of a term w_k acting as a zero-mean additive noise on the system dynamics, that is, $z_{k+1} = z_k + hF(z_k,u_k) + w_k$, and P_k is a covariance estimate for the current state estimate $\hat{z}_k$. The matrix R is the covariance matrix of a zero-mean additive measurement noise n_k, that is, $y_k = Cz_k + n_k$. The estimates of the EKF as in (15) are expected to converge to the extent the initial estimate $\hat{z}_0$ is sufficiently close to the actual initial state.

At time k_j we linearize the discrete time model (14) around the current estimated state $\hat{z}_{k_j}$ and input u_{k_j} to arrive at the following affine dynamical model

$$z_{k+1} = A_{k_j}z_k + B_{k_j}u_k + f_{k_j}, \quad (17)$$

for $k{>}k_j$, where A_{k_j}, B_{k_j} and f_{k_j} are functions of $\hat{z}_{k_j}$ and u_{k_j} as $A_{k_j} = I + h\left.\frac{\partial F}{\partial z}\right|_{(\hat{z}_{k_j}, u_{k_j})}$, $B_{k_j} = h\left.\frac{\partial F}{\partial u}\right|_{(\hat{z}_{k_j}, u_{k_j})}$, and $f_{k_j} = \hat{z}_{k_j} + F(\hat{z}_{k_j}, u_{k_j})$. The linearization is updated every N_l sampling periods, that is $k_j = jN_l$ and the resulting, time-varying, estimated system matrices are given to the MPC controller.

IV. Hybrid Modeling & Predictive Control

A. Hybrid Modeling

In this section we model the hybrid behaviour of the actuators using the *mixed logic and dynamics* framework [20]. The torques exerted by the thrusters are subject to a *minimum impulse bit* (MIB), meaning that, once the thrusters are switched on they cannot be turned off immediately and there is a fixed minimum period of time for which they remain open. This entails a minimum exerted torque on the corresponding axis which can be modeled by constraints of the form $u_k \in \mathcal{U}$, with

$$\mathcal{U} = [-u_{\max}, -u_{\min}] \cup \{0\} \cup [u_{\min}, u_{\max}], \quad (18)$$

where $u_{\min} \in \mathbb{R}^3$ denotes the minimum impulse bit and $u_{\max} \in \mathbb{R}^3$ denotes the maximum torque that can be provided in a sampling interval on each axis. In order to

translate this constraint to a computationally tractable form, we consider the convex constraints

$$-u_{\max} \leq u_k \leq u_{\max}, \tag{19}$$

introduce the binary vectors $\delta_k \in \{0,1\}^3$ and $\theta_k \in \{0,1\}^3$ which are written as $\delta_k = [\delta_k^1, \delta_k^2, \delta_k^3]'$ and $\theta_k = [\theta_k^1, \theta_k^2, \theta_k^3]'$, and we establish the correspondence

$$\delta_k^i = [u_i(k) \leq -u_{\min,i}] \text{ and } \theta_k^i = [u_i(k) \geq u_{\min,i}], \tag{20}$$

for $i = 1,2,3$. Notice that whenever $\delta^i = 1$ or $\theta^i = 1$, the control action u is outside the bounds defined by $\{u \mid -u_{\min} \leq u \leq u_{\min}\}$, so in light of (19) it can be applied to the system. We define the following propositional logic constraints on the auxiliary continuous variables $\eta_k \in \mathbb{R}^3$:

$$\eta_{i,k} = u_{i,k} \cdot [\delta_k^i \vee \theta_k^i], i \in \{1,2,3\} \tag{21}$$

where $\vee$ denotes the logical disjunction (OR) operator; clearly $\eta_k \in \mathcal{U}$. We introduce the auxiliary variables $v_k \in \mathbb{R}^3$ to trace whether a thruster activation takes place at time k

$$v_{i,k} = [\delta_k^i \vee \theta_k^i], i \in \{1,2,3\} \tag{22}$$

The system dynamics subject to the thrusters constraints can be described by the linear discrete-time model

$$z_{k+1} = Ax_k + B\eta_k + f \tag{23a}$$
$$\gamma_{k+1} = \gamma_k + \begin{bmatrix} 1 & 1 & 1 \end{bmatrix} v_k, \tag{23b}$$

where the additional state variable $\gamma_k \in \mathbb{R}$, namely the *activation count*, if necessary, can be bounded by the number of maximum activations allowed $\gamma_{\max}$ according to:

$$\gamma_k \leq \gamma_{\max}. \tag{24}$$

This constraint is likely to become active only if the prediction horizon is long enough to foresee the exhaustion of available actuations or γ_k is close to $\gamma_{\max}$. In (23a), A, B and f are provided by the linearization step explained in Subsection III.

B. Model Predictive Control

MPC is an optimization-based control methodology where at each time instant a performance index is optimized using a discrete-time model of the controlled process taking into account the constraints on the state and input variables of the system. This optimization yields a sequence of control actions whose first element is applied to the system as input while other elements are discarded [21]. As already mentioned, the proposed control scheme aims at (i) steering the pitch and yaw errors and the spin rate to desired set-points while (ii) accounting for the aforementioned constraints and (iii) exhibiting a sparse actuation profile.

The model used by MPC here is an affine model of the system obtained by linearization and the proposed hybrid MPC

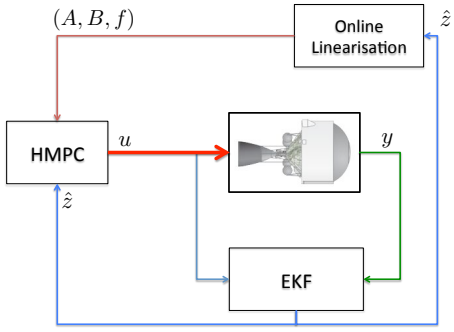

Fig. 3: The proposed control scheme with the hybrid MPC controller, the EKF and the online linearization.

scheme, illustrated in Figure 3, is formulated as follows:

$$\mathbb{P}(x_0, \gamma_0, A, B, f) : \min_{\pi_N} \quad V_N(\pi_N, \gamma_0) \tag{25a}$$
$$\text{s.t.} \quad x(0) = x_0, \ \gamma(0) = \gamma_0, \tag{25b}$$
$$\text{Constraints (19) – (24), for } k \in \mathbb{N}_{[0,N_u]}, \tag{25c}$$
$$z_{k+1} = Az_k + B\eta_k + f, \ \text{for } k \in \mathbb{N}_{[N_u,N-1]}, \tag{25d}$$
$$-u_{\max} \leq \eta_k \leq u_{\max}, \ \text{for } k \in \mathbb{N}_{[N_u,N-1]} \tag{25e}$$

where $N_u \leq N$ defines the *hybrid control horizon*, *i.e.*, the number of time steps for which the minimum impulse bit is taken into account as in (25c). Let us denote the set of optimization variables of the MPC problem by $\pi_N = \{\{u_k, v_k, \delta_k\}_{k \in \mathbb{N}_{[0,N_u]}}, \{\eta_k\}_{k \in \mathbb{N}_{[0,N-1]}}\}$, where $N \geq 1$ is the *prediction horizon* and let x_0 be the current state, γ_0 be the total number of activations up to the current time instant k and let A, B and f be estimated linearization matrices of the system derived as in Section III. The MPC control action is computed in a *receding horizon* fashion: At every sampling time instant, optimization problem (25) is solved to yield the optimal solution $\pi_N^\star$ and the first control action $\eta_0^\star$ is applied to the system. The MPC controller commands admissible torques to the thrusters which will be activated for a certain time between $t_{\min}$ and T_s, where $t_{\min}$ is the minimum time for which the thrusters can remain open (and corresponds to a u_{min} torque) and T_s is the sampling time. The proposed methodology accounts for the hybrid nature of the thrusters and offers a clear advantage over other approaches to attitude control that issue merely on/off commands [22]. In fact, with the proposed approach the sampling time T_s can be much larger than the minimum impulse time $t_{\min}$, as a result, the MPC controller can have a greater foresight of the system evolution at a much lower computational cost.

A short hybrid control horizon compared to the prediction horizon is typically employed to reduce the complexity of the resulting optimization problem. In the proposed formulation (25), the input is assumed to satisfy all constraints given by equations (19)–(24) for all $k \in \mathbb{N}_{[0,N_u]}$. For time instants after N_u, we relax the hybrid constraints and we assume that the input can take any value subject to the constraints (25e) and the system dynamics (25d).

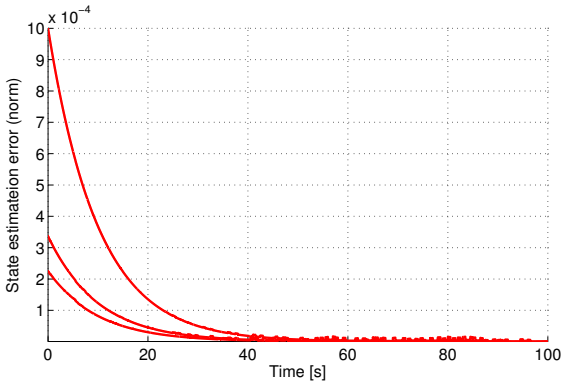

Fig. 4: Norm of the observer error for various initial state estimates $\hat{z}_0$.

For the chosen sampling time of $0.5s$, a large prediction horizon is required for the MPC controller to have enough foresight given that the rotational dynamics of the upper stage is relatively slow. The computational complexity can be mitigated by choosing a short hybrid control horizon.

The cost function V_N in (25) is defined as

$$V_N(\pi_N, \gamma_0) = V_f(z_N, \gamma_N) + \sum_{k=0}^{N-1} \ell(z_k, \eta_k) \qquad (26)$$

where ℓ is the stage cost $\ell(z,u) = \|Qz\|_p + \|Ru\|_p$, and V_f is the terminal cost defined as $V_f = \|Q_N z_N\|_p + \rho(\gamma_N - \gamma_0)$.

Matrices Q, Q_N, R and ρ are used to strike a desired trade-off between pointing accuracy and usage of thrusters. Any p-norm ($1 \leq p \leq \infty$) can be used for the stage and terminal cost functions. Here we used $p = \infty$ so that the resulting problem is a mixed-integer linear problem (MILP).

V. Simulation Results

Firstly we assess the performance of the EKF observer. We define the observer error as $e_k = z_k - \hat{z}_k$. The norm of e_k for different initial state estimates is presented in Figure 4. The observer, tested in closed-loop with the proposed hybrid MPC controller, was found to converge in a small neighbourhood about the actual state of the system.

In order to assess the performance of the closed-loop system using different tuning parameters we introduce certain performance indicators. First, the *pointing-accuracy indicator*

$$J_{\text{pa}}^{K} = \sum_{k=T_{\text{sim}}-K}^{T_{\text{sim}}} \epsilon_{y,k}^2 + \epsilon_{z,k}^2, \qquad (27)$$

where T_{sim} is the simulation time and K is the number of time instants before the end of the simulation to be considered. We also introduce the *total squared error indicator*

$$J_{\text{tse}} = \sum_{k=0}^{T_{\text{sim}}} \epsilon_{y,k}^2 + \epsilon_{z,k}^2, \qquad (28)$$

the number of thruster actuations along the y and z axes, denoted by J_{act}^{y} and J_{act}^{z} and the total actuation count on the y and z axes, J_{act}. In all cases ω_x converges fast to its set-point with few actuations along the x axis (see for example Figures 6 and 7).

TABLE I: Evaluation of the closed-loop performance by simulations over a period $T_{\text{sim}} = 300\text{s}$.

ρ	J_{act}^{y}	J_{act}^{y}	J_{act}	J_{pa}^{40}	J_{tse}
0.005	37	131	168	$1.14 \cdot 10^{-4}$	0.0510
0.05	28	56	84	0.0018	0.0834
0.1	32	48	80	0.0349	0.2988
0.2	34	45	79	0.1279	1.6862

In Table I we summarise the evaluation results of the closed-loop system for different values of ρ having fixed $Q = \text{diag}(7,7,4,1,1,1,1)$, $Q_N = 2Q$, $R = 0$ and $p = \infty$. The linearization is updated with $N_l = 10$, *i.e.*, every $5s$. The prediction horizon is fixed to $N = 20$ and $N_u = 8$; this particular choice of the prediction and hybrid control horizon was found to offer a good trade-off between optimality and computational complexity. It is interesting to see that if we decrease the hybrid control horizon to $N_u = 2$, the pointing accuracy worsens significantly leading to $J_{\text{pa}}^{40} = 1.1669$ and $J_{tse} = 52.98$ with $J_{\text{act}} = 144$. The respective simulations are presented in Figure 8. This important observation justifies the use of hybrid MPC for the control of spacecraft with impulsive thrusters. Moreover, hybrid control horizon values larger than 8 were not found to improve the closed-loop performance, thus, were avoided for the sake of retaining the complexity as low as possible. The average computation time for the derivation of the control action was $0.12s$ on a $2.2GHz$ Intel Core i7 machine. Simulations were carried out in MATLAB 2013a, using YALMIP [23] and the MILP solver of Gurobi.

We can notice that higher values of ρ lead to a sparser actuation profile reducing the number of y and z actuations at the cost of a lower pointing accuracy and overall performance (in terms of J_{pa} and J_{tse}). The state trajectory for $\rho = 0.05$ is illustrated on the ϵ_y-ϵ_z-plane in Figure 5 where we observe that the state moves into a small neighbourhood of the set-point. The HMPC commands are shown in Figure 6 and the spin rate is presented in Figure 7.

References

[1] J. Wertz, ed., *Spacecraft attitude determination and control*. Dordrecht: Kluwer Academic Publishers, 1978.

[2] R. Ibrahim, *Liquid sloshing dynamics*. Cambridge: Cambridge university press, 2005.

[3] P. Hughes, *Spacecraft attitude dynamics*. Dover Publications Inc., 1986.

[4] A. Veldman and M. Vogels, "Axisymmetric liquid sloshing under low-gravity conditions," *Acta Astronautica*, vol. 11, no. 10–11, pp. 641 – 649, 1984.

[5] J. Hervas and M. Reyhanoglu, "Thrust-vector control of a three-axis stabilized upper-stage rocket with fuel slosh dynamics," *Acta Astronautica*, vol. 98, no. 0, pp. 120 – 127, 2014.

[6] V. Manikonda, P. Arambel, M. Gopinathan, R. Mehra, and F. Hadaegh, "A model predictive control-based approach for spacecraft formation keeping and attitude control," in *American Control Conference*, vol. 6, pp. 4258–4262, 1999.

[7] M. Vieira, R. Galvao, and K. Heinz Kienitz, "Attitude stabilization with actuators subject to switching-time constraints using explicit MPC," in *IEEE Aerospace Conference*, pp. 1–8, 2011.

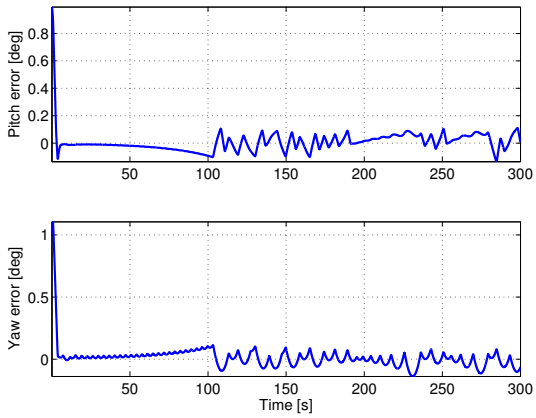

Fig. 5: Controlled trajectory in the time domain with EKF and HMPC in the loop for $300s$ with $\rho = 0.05$.

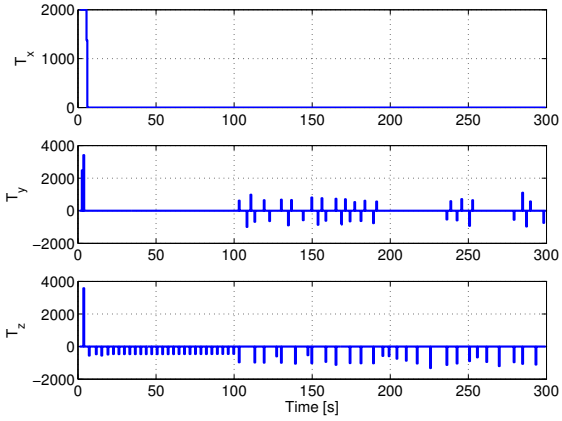

Fig. 6: Torques (in Nm) applied by the impulsive thrusters ($\rho = 0.05$).

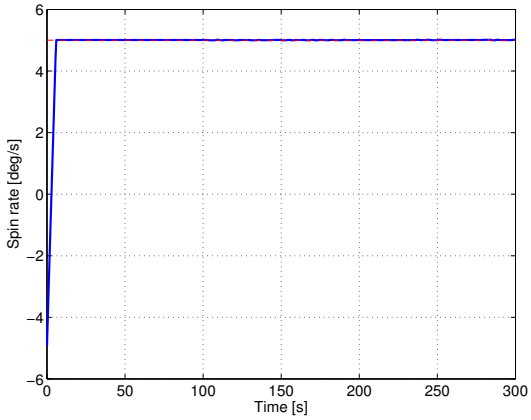

Fig. 7: Spacecraft in barbecue mode: the spin rate ω_x tracks the desired set-point.

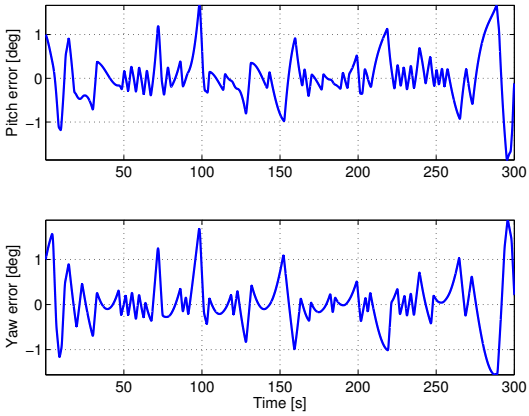

Fig. 8: Closed-loop trajectory with $N = 20$ and $N_u = 2$.

[8] Ø. Hegrenæs, J. Gravdahl, and P. Tondel, "Attitude control by means of explicit model predictive control, via multi-parametric quadratic programming," in *American Control Conference*, pp. 901–906 vol. 2, 2005.

[9] Ø. Hegrenæs, J. Gravdahl, and P. Tondel, "Spacecraft attitude control using explicit model predictive control," *Automatica*, vol. 41, no. 12, pp. 2107 – 2114, 2005.

[10] A. Kater, "Attitude Control of Upper Stage Launcher During Long Coasting Period," Master's thesis, Lehrstuhk f ur Automatisierungs- und Regelungstechnik, Christian-Albrechts-University Kiel, Germany, 2013.

[11] S. Beatty, "Comparison of PD and LQR methods for spacecraft attitude control using star trackers," in *World Automation Congress*, pp. 1–6, 2006.

[12] U. Kalabic, R. Gupta, S. Di Cairano, A. Bloch, and I. Kolmanovsky, "Constrained spacecraft attitude control on SO(3) using reference governors and nonlinear model predictive control," in *American Control Conference*, pp. 5586 – 5593, IEEE, June 2014.

[13] A. Richards, J. How, T. Schouwenaars, and E. Feron, "Plume avoidance maneuver planning using mixed integer linear programming," in *Proc. of AIAA Guidance, Navigation, and Control Conf.*, (Montreal, Canada), Aug. 2001.

[14] D. Mellinger, A. Kushleyev, and V. Kumar, "Mixed-integer quadratic program trajectory generation for heterogeneous quadrotor teams," in *IEEE Conf. Robotics and Automation*, pp. 477–483, May 2012.

[15] P. Patrinos, A. Guiggiani, and A. Bemporad, "Fixed-point dual gradient projection for embedded model predictive control," in *Proc. 12th European Control Conference*, (Zurich, Switzerland), 2013.

[16] A. Guiggiani, I. Kolmanovsky, P. Patrinos, and A. Bemporad, "Fixed-point constrained model predictive control of spacecraft attitude." arXiv:1411.0479, 2014.

[17] D. Frick, A. Domahidi, and M. Morari, "Embedded Optimization for Mixed Logical Dynamical Systems," *Computers & Chemical Engineering*, July 2014. to appear.

[18] D. Wells, *Lagrangian Dynamcis*. McGraw-Hill, 1967.

[19] A. Weiss, I. Kolmanovsky, M. Baldwin, and R. S. Erwin, "Model predictive control of three dimensional spacecraft relative motion," in *American Control Conference*, (Montreal, Canada), pp. 173–178, 2012.

[20] A. Bemporad and M. Morari, "Control of systems integrating logic, dynamics, and constraints," *Automatica*, vol. 35, no. 3, pp. 407 – 427, 1999.

[21] J. B. Rawlings and D. Q. Mayne, *Model Predictive Control: Theory and Design*. Nob Hill Publishing, 2009.

[22] M. Leomanni, A. Garulli, A. Giannitrapani, and F. Scortecci, "An MPC-based attitude control system for all-electric spacecraft with on/off actuators," in *52th IEEE Conf. on Decision and Control*, (Florence, Italy), pp. 4853–4858, 2013.

[23] J. Löfberg, "YALMIP : a toolbox for modeling and optimization in matlab," in *Computer Aided Control Systems Design*, pp. 284–289, Sept 2004.